Solar Deflection of Thin-Walled Cylindrical, Extendible Structures

ROBERT J. EBY* AND ROBERT D. KARAM†
Fairchild Hiller Corporation, Space and Electronics Systems Divison, Germantown, Md.

An analytical expression is derived which describes the steady-state deflection of a long, thin, tubular structure with a locked overlapped cross section subjected to solar heating in a 0 g environment. By transforming the angular coordinate to correspond to the solar direction, it is possible to obtain a single expression which describes the circumferential temperature distribution. Thermal bending is found by closed form integration of the temperature-induced loading about the principal axes as dictated by overlap geometry. Maximum thermal bending is evaluated for various overlap angles as a function of dimensionless groups which include all thermal and geometric parameters. It is concluded that an optimum design is one which incorporates an overlap angle at 155°. The results are presented in graphical form suitable for engineering design, and a specific example is discussed.

Nomenclature

a = cross-sectional area of tube
A = temperature parameter
B = dimensionless parameter
e = thermal coefficient of expansion
E = Young's modulus of elasticity
$f(\theta_s)$ = function defined by Eq. (16)
F = heat input function
I = area moment of inertia
k = thermal conductivity
M = thermal bending moment
r = element radius
S = solar flux
t = element thickness
T = absolute temperature
u = transformed dimensionless temperature
x,y = position coordinates on circumference
Z = position along longitudinal axis
α = solar absorptivity
δ = deflection
ϵ = emissivity
η = temperature fluctuation function
θ = angular position on circumference
σ = Stefan-Boltzmann constant
τ = dimensionless temperature defined by Eq. (9)
ϕ = overlap angle
ψ = transformed angular position
Ω = angle of misalignment with solar line

Subscripts

s = position of maximum normal component of solar vector
x,y = along X axis and Y axis, respectively
0 = reference value
av = average
max = maximum

Introduction

TUBULAR Extendible Elements (TEE's) are being employed for a variety of scientific and technologicl purposes such as gravity gradient stabilization, dipole antennas and instrumentation extension systems. Recently, they have been put to use as extremely long antennas in radio astronomy and electric field measurement satellites.

Received January 29, 1969; revision received December 10, 1969. The authors wish to express their appreciation to W. H. Kelly of Fairchild Hiller for consultation and for his effort in obtaining and graphing the results.

* Manager, Thermal Control.

† Principal Engineer, Thermal Control.

The TEE's are usually thin, metallic ribbons which are rolled into tubes (along their longitudinal axis) and heat treated. The tubes are then opened, flattened into a ribbon again and wound on a small diameter motor driven spool. When an element is extended, it takes the form of a tube with circular cross sections and overlapped edges as shown schematically in Figs. 1a and 1b. Torsional rigidity is enhanced by the use of a seam of interlocking tabs.

In many space applications, the main area of concern is the effect of the added structure on the vehicle earth tracking dynamics. In others, such as instrumentation extension systems, the experimenter requires accurate predictions concerning the tube configuration in the space environment. In either case, thermal bending induced by solar radiation is of prime importance.

Florio and Hobbs[1] investigated the temperature distribution in overlapped gravity gradient rods. The problem of deflection of thin-walled cylinders of open section has been discussed by Frisch.[2] Koval, Mueller, and Paroczai[3] formulated a mathematical model to describe the flutter of overlapped booms excited by a thermal load.

The mathematical treatment of the deflection of open section cylinders is complicated by the presence of torsional twist and frictional effects along the overlap surface of contact. By making the zero twist assumption, which is justified when interlocking tabs are employed, the mathematical analysis is greatly simplified and the results can be readily investigated in terms of the effect of the geometric parameters on deflection.

An analytical solution which allows direct computation of the spacial coordinates of the deflected longitudinal axis for any orientation with respect to the sun is presented. Maxi-

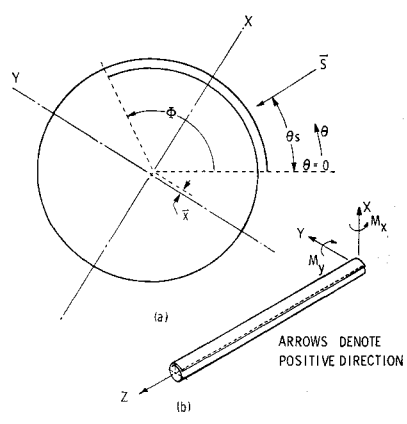

Fig. 1 Coordinate system.

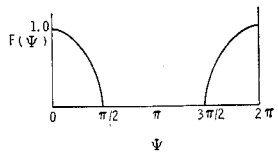

Fig. 2 Solar input function.

mum bending is evaluated as a function of the overlap angle and the thermal-mechanical properties of the element.

Assumptions

1) The element is a long homogeneous cantilevered thin shell of overlapped circular cross section with constant thermal and mechanical properties.

2) The position of the overlap with respect to solar direction does not vary along the length. Hence, there is no longitudinal temperature variation

3) The effects of internal radiation and thermal interchange within the gap of the overlapped sector are insignificant.

4) The form of the solar input function is a rectified cosine wave.

5) The temperature at any point does not vary significantly from an average circumferential temperature.

6) An elemental length is equal to its projection and the square of the slope of the deflected shape is small compared to unity.

The first assumption is valid by virtue of the physical construction of elements of the type discussed in the Introduction. In addition, the surface finish or coating used in practice results in temperatures which are well below the values at which the material properties begin to deviate from their nominal values.

The second assumption implies the absence of torsional displacements along the tube length. Under many circumstances this is only valid for tubes which employ locked seams, i.e., for open slit tubes thermal bending is usually accompanied by twist which causes the position of the overlap to vary along the length. However, early difficulties experienced with the attitude dynamics of satellites using open slit tubes have all but precluded their use for missions planned in the future.[3] Various techniques for achieving an interlock at the seam have been developed, flight qualified, and are generally accepted.

Assumption three, neglecting the reduction in the circumferential temperature gradient due to internal radiation and thermal interchange across the overlap, will lead to slightly conservative values of deflection.

The fourth assumption restricts the input function to a rectified cosine wave. This approximates the solar heat input. The solution can be extended to include planetary irradiation as well as the effect of solar absorptance (α) variation with solar incidence angle.[4]

The fifth assumption is necessary for linearizing the energy equation. Linearization does not introduce significant errors in the thermal deflection equations which depend on temperature gradient rather than temperature magnitude. (See Results and Observations.)

Assumption six allows the use of small deflection theory in predicting thermal bending. This is perhaps the least valid of the assumptions when very long tubes are considered. It may be noted, however, that for 0.5 in. diam, 0.002 in. wall continuous beryllium-copper tube, the error in the resultant deflection is less than 2% for lengths up to 300 ft.[5]

Analysis

The coordinate system is shown in Figure 1 in which $\theta = 0$ coincides with the outer edge of the overlap. The location of the principal axes depends on the angle ϕ subtended by the overlap. X is the symmetry axis which bisects the overlapped sector and passes through the geometric center. The Y axis is normal to it and displaced from the geometric center by the distance $\bar{x}$. From the definition of the centroid, $\bar{x}$ is given by

$$\bar{x} = \frac{\int_a x'da}{\int_a da}$$

where x' is measured from the geometric center. Hence,

$$\bar{x} = (r \sin\phi/2)/(\pi + \phi/2) \tag{1}$$

A point on the circumference is given by the coordinates

$$x = r[\cos(\theta - \phi/2) - (\sin\phi/2)/(\pi + \phi/2)] \tag{2}$$

$$y = r \sin(\theta - \phi/2) \tag{3}$$

Therefore, the geometrical moments of inertia about the principal axes are

$$I_x = \int_0^{2\pi+\phi} ty^2 r d\theta = r^3 t \left[\pi + \frac{\phi}{2} - \frac{\sin\phi}{2}\right] \tag{4}$$

$$I_y = \int_0^{2\pi+\phi} tx^2 r d\theta = r^3 t \left[\pi + \frac{\phi}{2} + \frac{\sin\phi}{2} - \frac{2\sin^2\phi/2}{\pi + \phi/2}\right] \tag{5}$$

The direction of the sun is denoted by θ_s.

The differential equation which relates the steady-state circumferential heat conduction to that which is received and reradiated to space may be written

$$d^2T/d\theta^2 + (\alpha S r^2/kt)F(\theta) - (\epsilon r^2/kt)\alpha T^4 = 0 \tag{6}$$

$$0 \leq \theta \leq 2\pi$$

$$d^2T/d\theta^2 = 0, \ \theta \geq 2\pi \tag{7}$$

The function $F(\theta)$ in Eq. (6) characterizes the component of a unit solar vector incident normal to the surface element. Thus, for example, if the sun is normal to $\theta = 0$ then $F(\theta)$ has the form shown in Fig. 2.

Edge heat losses are assumed negligible (thin shell) hence the boundary conditions of the problem may be taken as $dT/d\theta = 0$ at $\theta = 0$ and $\theta = 2\pi + \phi$. An immediate consequence of these conditions is that the temperature is a constant for $\theta \geq 2\pi$ and hence $dT/d\theta = 0$ at $\theta = 2\pi$.

Eq. (6) is nonlinear and no known exact solution is available. Following Charnes and Raynor,[6] the following definition is introduced:

$$T = T_{av}(1 + \eta), \ |\eta| \ll 1 \tag{8}$$

Further, define a dimensionless temperature

$$\tau = \eta + \tfrac{1}{4} \tag{9}$$

Neglecting higher powers of η, T^4 may be replaced by $4T_{av}{}^4\tau$.

The error introduced by linearization may be reduced by defining T_{av} as the effective temperature which satisfies the condition that in steady state the integrated absorbed solar flux is equal to the heat radiated at T_{av}. That is

$$2\pi r\epsilon\sigma T_{av}{}^4 = \int_0^{2\pi} \alpha S r F(\theta) d\theta$$

or

$$\alpha T_{av}{}^4 = \alpha S/\pi\epsilon \tag{10}$$

Equation (10) can be shown to be consistent with the definition of the average temperature given by

$$T_{av} = \left(\frac{1}{2\pi}\right) \int_0^{2\pi} T(\theta) d\theta \tag{11}$$

The form of the function $F(\theta)$ suggests a solution by the

method of Laplace Transformation. The analysis is facilitated by introducing the transformations $\tau = u + \tau_s$ and $\theta = \psi + \theta_s$ where τ_s is a dimensionless temperature at θ_s. $F(\theta)$ becomes now $F(\psi)$ and is given by Fig. 2 regardless of the position of the sun. The solution of the linearized equation with boundary conditions $du/d\psi = 0$ at $\psi = -\theta_s$ and $\psi = 2\pi - \theta_s$ gives after some manipulation;

$$\frac{T(\theta)}{A} = \frac{4}{\pi B} + \frac{1}{2(B+1)}\cos(\theta - \theta_s) - \frac{1}{8\pi}\sum_{n=1}^{\infty}\frac{(-1)^n \cos 2n(\theta - \theta_s)}{(n^2 - \frac{1}{4})(n^2 + B/4)} + f(\theta_s)[\cosh B^{1/2}\theta - \cosh B^{1/2}(2\pi - \theta)], \quad 0 \le \theta \le 2\pi \tag{12}$$

$$\frac{T(\theta)}{A} = \frac{T(2\pi)}{A} = \frac{4}{\pi B} + \frac{1}{2(B+1)}\cos\theta_s - \frac{1}{8\pi}\sum_{n=1}^{\infty}\frac{(-1)^n \cos 2n\theta_s}{(n^2 - \frac{1}{4})(n^2 + B/4)} + f(\theta_s)[\cosh B^{1/2}2\pi - 1], \quad \theta \ge 2\pi \tag{13}$$

where

$$A = \alpha S r^2/kt \tag{14}$$

$$B = 4\epsilon r^2 \alpha T_{av}^3/kt \tag{15}$$

and

$$f(\theta_s) = \frac{1}{B^{1/2}\sinh B^{1/2}\,2\pi} \times \left[\frac{1}{4\pi}\sum_{n=1}^{\infty}\frac{(-1)^n n \sin 2n\theta_s}{(n^2 - \frac{1}{4})(n^2 + B/4)} - \frac{\sin\theta_s}{2(B+1)}\right] \tag{16}$$

The average temperature defined by Eq. (11) can be evaluated by using Eq. (12) and is found to satisfy Eq. (10).

The unsymmetrical temperature distribution causes a deflection of the element due to the difference in the relative expansion of the longitudinal fibers. This deflection may be considered as the result of equivalent thermal moments about the principal axes which would be required to suppress the element from deforming. Based on the coordinate system described in Fig. 1, the thermal moments are represented by[7]

$$M_x = \int_a eETy\,da \tag{17}$$

$$M_y = -\int_a eETx\,da \tag{18}$$

where e is the coefficient of thermal expansion and E is the modulus of elasticity. The integration is taken over the cross section of elemental area da.

Changing to cylindrical coordinates by using Eqs. (2) and (3) and substituting for T the expressions given by Eqs. (12) and (13), the dimensionless thermal bending moments are obtained:

$$\frac{M_x}{M_0} = \frac{2(1 - \cosh B^{1/2}2\pi)\cos\phi/2}{B+1} f(\theta_s) + \frac{\pi}{2(B+1)} \times \sin\left(\theta_s - \frac{\phi}{2}\right) \tag{19}$$

$$\frac{M_y}{M_0} = \frac{2(\phi - 2\pi B)(\cosh B^{1/2}\,2\pi - 1)\sin\phi/2}{(2\pi + \phi)(B+1)} f(\theta_s) - \frac{\pi}{2(B+1)}\cos\left(\theta_s - \frac{\phi}{2}\right) + \frac{2\pi \sin\phi/2}{2\pi + \phi} \times \left[\frac{1}{4\pi}\sum_{n=1}^{\infty}\frac{(-1)^n \cos 2n\theta_s}{(n^2 - \frac{1}{4})(n^2 + B/4)} - \frac{\cos\theta_s}{B+1}\right] \tag{20}$$

where $M_0 = AeEr^2t$ and $f(\theta_s)$ is given by Eq. (16). The deflection is obtained from Bernoulli-Euler equation with the moment equal to a constant along the cantilivered element:

$$\frac{\delta_x}{\delta_0} = \frac{\frac{1}{2}(M_y/EI_y)Z^2}{\frac{1}{2}(M_0/EI_0)Z^2} = \left(\frac{I_0}{I_y}\right)\left(\frac{M_y}{M_0}\right) \tag{21}$$

$$\frac{\delta_y}{\delta_0} = \frac{\frac{1}{2}(M_x/EI_x)Z^2}{\frac{1}{2}(M_0/EI_0)Z^2} = \left(\frac{I_0}{I_x}\right)\left(\frac{-M_x}{M_0}\right) \tag{22}$$

δ_x and δ_y are the deflections in the positive X and positive Y directions, respectively. $\delta_0 = \frac{1}{2}(M_0/EI_0)Z^2$ and $I_0 = (I_x^2 + I_y^2)^{1/2}$.

In general, the deflection is not aligned with the sun direction. If Ω is defined as the angle between the solar vector and the displacement vector, then

$$\Omega = \tan^{-1}(\delta_y/\delta_x) - (\theta_s - \phi/2) - 180° \tag{23}$$

Results and Observations

1. Linearization

In order to evaluate the inaccuracies introduced by linearization, a nodal network thermal balance computer program was used to obtain a solution of Eq. (6). Two sets of values were chosen for α, ϵ, k, r, and t which exceed the limits of the range of values applicable to commonly used elements. The temperature distributions as compared to the analytical solution of the linearized equation are shown in Figs. 3a and 3b for two sun locations. It is seen that for small values of B, the approximate solution is very close to the computer solution. For large values of B, the temperature deviates noticeably from the computer value but neither the shape of the profile nor the gradients are significantly different. Hence, the analytical expressions for thermal bending moments, Eqs. (19) and (20), remain approximately correct. Furthermore, in most applications the value of B is at least an

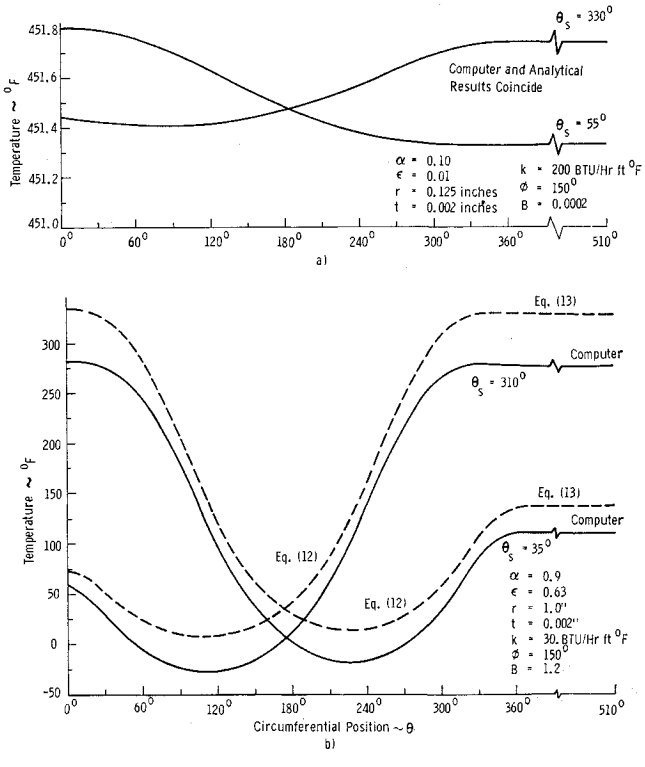

Fig. 3 Temperature profile-comparison between linearized equation and computer results.

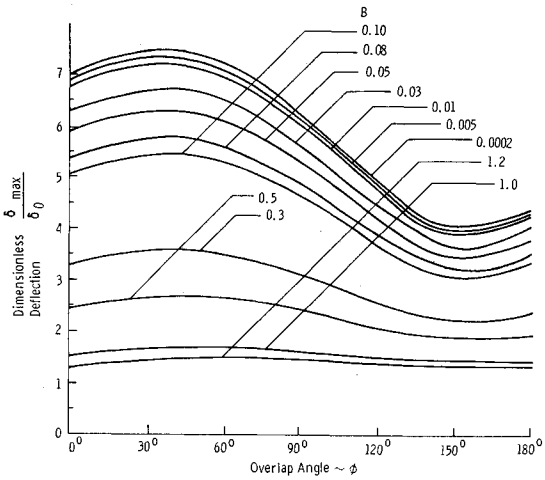

Fig. 4 Maximum dimensionless deflection.

order of magnitude less than that indicated in Fig. 3b which makes the use of the analytical expressions quite valid.

It can be deduced from Eqs. (19) and (20) that both M_x and M_y (but not necessarily M_x/M_0 and M_y/M_0) tend to vanish when B is made very small. ($B \rightarrow 0$) This is consistent with the physical fact that for elements of small radii and high conductivity, the thermal gradients are small.

2. Convergence of Series

The summation terms in Eqs. (12) and (13) may be replaced by closed-form expressions once the regions of θ and $\theta - \theta_s$ are specified. A set of six equations would then be obtained to define the circumferential temperature distribution.[1] However, the fact that the series converge rapidly for all values of θ and θ_s allows convenient engineering calculations of the temperature distribution as well as direct integration of the results to obtain the bending moment.

3. Continuous Cylindrical Shells

A special case of the temperature and moment equations is when both ϕ and θ_s are set equal to zero. This corresponds to the solution of the closed, continuous cylindrical shell. Two regions on the cylinder which are defined by I: $0 \leq \theta \leq \pi/2$ and II: $\pi/2 \leq \theta \leq \pi$ may be considered. For region I, the series[8]

$$\sum_{n=1}^{\infty} \frac{(-1)^n \cos 2n\theta}{(n^2 - \frac{1}{4})(n^2 + B/4)} = \frac{4}{B+1} \times \sum_{n=1}^{\infty} \left(\frac{(-1)^n \cos 2n\theta}{n^2 - \frac{1}{4}} - \frac{(-1)^n \cos 2n\theta}{n^2 + B/4} \right)$$

can be shown to converge to

$$-\frac{4}{B+1}\left[\pi \cos\theta - 2 + \frac{\pi \cosh B^{1/2}\theta}{B^{1/2} \sinh B^{1/2}\pi/2} - \frac{2}{B}\right]$$

Similarly, for region II the series converge to

$$-\frac{4}{B+1}\left[\pi \cos(\theta - \pi) - 2 + \frac{\pi \cosh B^{1/2}(\theta - \pi)}{B^{1/2} \sinh B^{1/2}\pi/2} - \frac{2}{B}\right]$$

When these results are incorporated into Eqs. (12) and (13), the dimensionless temperature distributions are obtained:

$$\frac{T_I}{A} = \frac{\cosh B^{1/2}\theta}{2B^{1/2}(B+1)\sinh B^{1/2}\pi/2} + \frac{\cos\theta}{B+1} + \frac{3}{\pi B} \quad (24)$$

$$\frac{T_{II}}{A} = \frac{\cosh B^{1/2}(\theta - \pi)}{2B^{1/2}(B+1)\sinh B^{1/2}\pi/2} + \frac{3}{\pi B} \quad (25)$$

Symmetry about the line $0 - \pi$ leads to immediate extension of the results to include the region $\pi \leq \theta \leq 2\pi$. The Equations for the thermal moments become

$$(M_x/M_0)\ \text{cylinder} = 0 \quad (26)$$

$$(M_y/M_0)\ \text{cylinder} = -[\pi/2(B+1)] \quad (27)$$

The dimensionless deflection is given by Eq. (21) in which $I_0/I_y = 2^{1/2}$

$$(\delta/\delta_0)\ \text{cylinder} = -[\pi/2^{1/2}(B+1)] \quad (28)$$

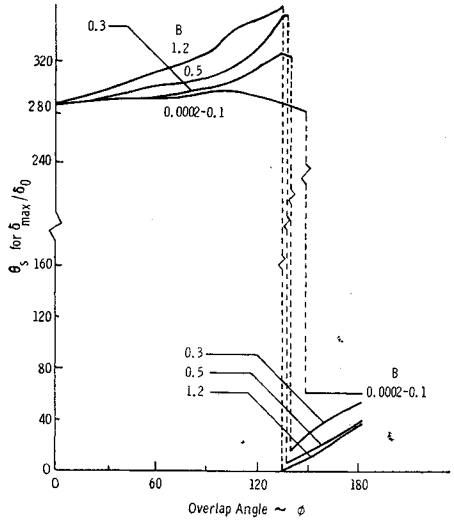

Fig. 5 Sun's position for maximum dimensionless deflection.

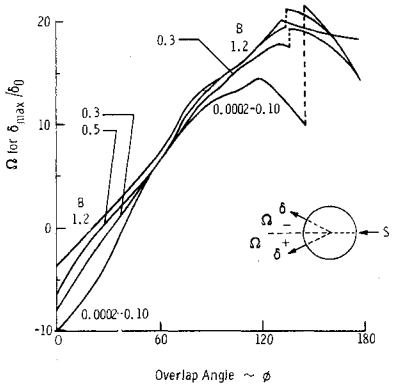

Fig. 6 Out-of-sunline angle for maximum dimensionless deflection.

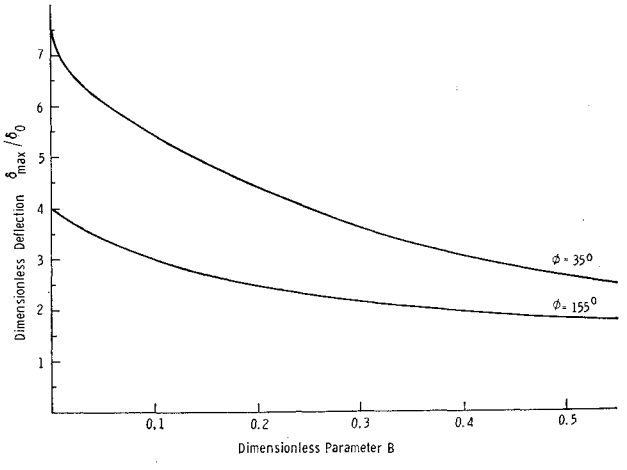

Fig. 7 Deflection vs B.

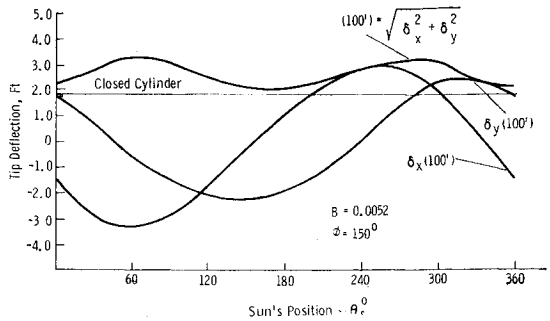

Fig. 8 Tip deflection vs. sun's position, $B = 0.0052$, $\phi = 150°$, length = 100 ft.

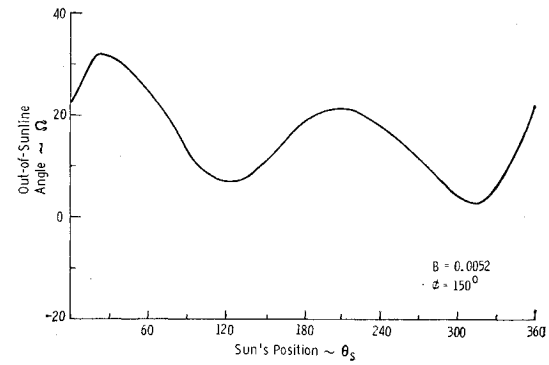

Fig. 9 Direction of deflection, $B = 0.0052$, $\phi = 150°$.

From the definitions of, δ_0, I_0, and B, the deflection is found to be

$$\delta \text{ cylinder} = -[e\alpha Sr/4(kt + 4\epsilon r^2\sigma T_{av}^3)]Z^2 \qquad (29)$$

and the displacement is in the direction of the solar vector, i.e., $\Omega = 0$.

4. Maximum Deflection

It is of interest from an engineering point-of-view to determine the maximum tip deflection of an element of given parameters. Equations (21) and (22) were numerically solved for various values of the overlap angle ϕ and the parameter B. The location of the solar vector, θ_s, was varied around the circumference and the maximum dimensionless deflection

$$\delta_{max}/\delta_0 = [(1/\delta_0)\,(\delta_x^2 + \delta_y^2)^{1/2}]_{max}$$

was plotted as shown in Fig. 4. For each value of B and ϕ there is a corresponding value of the solar angle which maximizes the deflection. This plot is shown in Fig. 5. The out-of-line deflection for maximum bending is given in Fig. 6. The dotted lines in these figures imply that θ_s (and hence Ω) can have two values for the same maximum dimensionless deflection. This occurs for overlap angles between 130° and 150°.

It is significant to note that for a given value of B, the maximum possible deflection is minimized when the overlap angle is chosen at about 155°. This angle corresponds to the configuration for which $I_x = I_y$ (the axes are principal central) and insures the coincidence of the shear center and geometric center. Hence, it is best for overlapped TEE's. Figure 7 shows the maximum dimensionless deflection as a function of B when $\phi = 155°$. For $\phi = 35°$, the deflection is a maximum for a given value of B.

Example

Consider the following data for a beryllium copper, 100 ft. long antenna with silver plating on the exterior surface. $\alpha = 0.10$, $\epsilon = 0.06$, $r = 0.25$ in., $t = 0.0015$ in., $k = 61$ Btu/ft hr °R, $e = 9.2 \times 10^{-6}$ in. per in./°R, $E = 18 \times 10^6$ psi, and $\phi = 150°$.

Assume solar radiation to be the only source of heat input and let $S = 440$ Btu/ft² hr From Eq. (10), $\alpha T_{av}^4 = 233.43$ Btu/ft² hr, hence $T_{av} = 607.4$°R and $\alpha T_{av}^3 = 0.384$. From Eqs. (14) and (15), $A = 2.504$°R and $B = 0.0052$. By definition: $M_0 = AeEr^2t = 0.0032$ lb. ft; from Eqs. (4) and (5), $I_x = 0.505 \times 10^{-8}$ ft⁴ and $I_y = 0.517 \times 10^{-8}$ ft⁴, hence $I_0 = (I_x^2 + I_y^2)^{1/2} = 0.723 \times 10^{-8}$ ft⁴, and $\delta_0(Z) = \frac{1}{2}(M_0/EI_0)Z^2 = 0.854(Z/100)^2$. From Fig. 4, the maximum dimensionless deflection corresponding to $\phi = 150°$ and $B = 0.0052$ is $\delta_{max}/\delta_0 = 3.9$, hence, the maximum tip deflection ($Z = 100$ ft) is δ_{max}(tip) $= 0.854 \times 3.9 = 3.33$ ft.

Figure 5 gives the position of solar vector that results in maximum deflection. θ_s(for maximum deflection) = 60°. The out-of-line displacement is given by Figure 6. Ω (for maximum deflection) = 21°.

Further insight is gained into the problem by evaluating Eqs. (21) and (22) for various positions of the solar vector as shown in Fig. 8. Comparison is made with the deflection of a closed cylinder of the same material, radius, and thickness. Figure 9 shows the direction of deflection with respect to the solar vector.

References

[1] Florio, F. A. and Hobbs, R. B., Jr., "An Analytical Representation of Temperature Distributions in Gravity Gradient Rods," *AIAA Journal*, Vol. 6, No. 1, Jan. 1968, pp. 99–102.

[2] Frisch, H. P., "Thermal Bending Plus Twist of a Thin-Walled Cylinder of Open Section with Application to Gravity Gradient Booms," TN D-4069, Aug. 1967, NASA.

[3] Koval, L. R., Mueller, M. R., and Paroczai, A. J., "Solar Flutter of a Thin-Walled Open-Section Boom," Symposium on Gravity Gradient Attitude Control, Aerospace Corp., El Segundo, Calif., Dec. 1968.

[4] Hoke, M. G., *A Thermal Vacuum Technique for Measuring the Thermal Absorptance of Satellite Coatings as a Function of Angle of Incidence*, NASA SP-55, 1965.

[5] Fixler, S., "Effects of Solar Environment and Aerodynamic Drag on Structural Booms in Space," *Journal of Spacecraft and Rockets*, Vol. 4, No. 3, March 1967, pp. 315–321.

[6] Charnes, A. and Raynor, S., "Solar Heating of a Rotating Cylindrical Space Vehicle," *ARS Journal*, Vol. 30, 1960, p. 479.

[7] Gatewood, B. E., *Thermal Stresses*, McGraw-Hill, New York, 1957, pp. 9–11.

[8] Jolley, L. B. W., *Summation of Series*, Dover, New York, 1961, p. 104.